Proceedings of ISFOG 2025
5TH INTERNATIONAL SYMPOSIUM ON
FRONTIERS IN OFFSHORE GEOTECHNICS
Nantes, France | June 9-13 2025

ISBN 978-2-85782-758-0

3D dynamic effective stress analyses of an offshore wind turbine on suction bucket jacket foundation under earthquake loading

Y. K. Chaloulos*
GR8 GEO, Athens, Greece

C. I. Tsifis, T.G. Limnaiou, P. Tasiopoulou, V. Drosos, A. Giannakou. J. Chacko
GR8 GEO, Athens, Greece

**ychaloulos@gr8-geo.com (corresponding author)*

ABSTRACT: The paper presents the development and application of an advanced 3D numerical methodology simulating the seismic response of an OWT supported on a three-legged suction bucket jacket (SBJ) foundation embedded in medium dense sands and silts. The methodology incorporates:1) the full jacket geometry and superstructure inertial characteristics by means of a properly calibrated system of beams, 2) a detailed 3D simulation of suction bucket foundations with shell elements, and 3) complex effective stress soil response simulated using the Ta-Ger constitutive model. Results show that the performance is governed by the formation of a zone of limited excess pore pressure build-up around the tip of the buckets, while they further highlight the importance of employing 3D advanced numerical analyses to facilitate performance-based design.

Keywords: Suction buckets, Earthquake, Jacket, Sands, Liquefaction

1 INTRODUCTION

Expansion of wind farms farther offshore, deeper water, and areas of high seismicity (e.g., Japan, Taiwan, California) pose new challenges in the design of OWT foundations. This is especially the case where the seabed comprises cohesionless materials prone to earthquake-induced liquefaction (e.g., sands and low plasticity silts). Where water depths or earthquake-related hazards become prohibitive for monopile foundations, jacket substructures are often considered to provide greater rotational restraint. Where soil conditions permit the installation of suction bucket jackets (SBJ) these represent an attractive alternative to relatively long conventional pile foundations. However, studies on seismic behavior of SBJs are generally limited (Farahani & Barari, 2023; Gao et al., 2022, 2023; Ueda et al., 2020; Yu et al., 2014) while current regulations do not incorporate design guidelines related to liquefaction.

The present paper presents the development and application of a novel 3D numerical methodology for the analysis of a three-leg Suction Bucket Jacket (SBJ) under seismic loading conditions. The methodology explicitly simulates the buckets, the jacket and the turbine while it also employs the Ta-Ger constitutive model to capture the response of the liquefiable soil layers.

2 SITE CONDITIONS

An idealized soil profile for a seismically active site with regular high magnitude earthquakes was developed for the study based on generic cone penetration test (CPT) and borehole data. Three idealised soils units were assumed for the study:

(a) Holocene sand unit (Unit-1) extending from seabed to about 7m depth primarily consisting of sands and silty sands with relative density D_r=48%,
(b) Holocene low plasticity silt unit (Unit-2) with *PI* values ranging between 2 and 6 encountered between ~7m and 25m depth. The silts in this unit are assumed to have tip resistances in the order of 2MPa. Unit-2 exhibits a sand-like behavior characterized by the development of significant excess pore pressures and liquefaction under cyclic loading
(c) Pleistocene unit (Unit-3) encountered at ~25m depth to the maximum depth explored of about 80 m primarily consisting of silty sands with D_r≈65% and occasional presence of clay layers less than 0.5 m thick.

Figure 1 shows idealized relative density D_r (Boulanger & Idriss, 2014) and small - strain shear wave velocity V_s (Andrus et al., 2007) profiles. It is noted that for the silts of Unit-2 relative density cannot meaningfully be measured in a lab. Nevertheless, the nominal relative density values estimated based on the procedure described above provided a useful basis for model calibration which was tied to characteristic CPT signatures. Hydraulic conductivity values for each layer were estimated based on the generic CPT data (Robertson, 2010) and were set equal to k=10^{-5}, 10^{-7} and 3x10^{-6}m/s for Unit-1, Unit-2 and Unit-3 respectively.

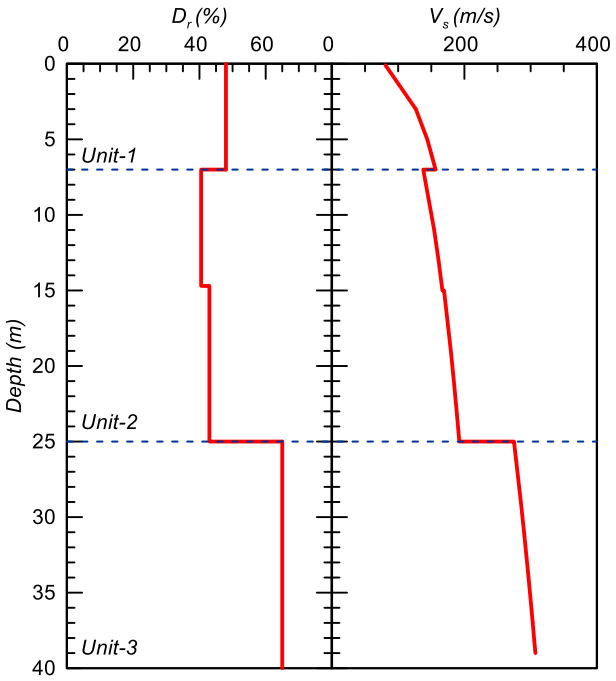

Figure 1. Idealized Relative density and small-strain shear wave velocity profiles

3 MODELING APPROACH

3D fully coupled effective-stress, dynamic Soil-Structure-Interaction (SSI) analyses including the soil, the buckets, the jacket, the tower and the Rotor Nacelle Assembly (RNA) were performed using the finite difference code FLAC3D v7.0 (Itasca, 2019). FLAC3D incorporates the ability to model groundwater flow and pore pressure dissipation, and adopts a *u-p* scheme for full coupling between the deformable porous soil skeleton and the water flowing within the pore space. It employs an explicit solution algorithm which is well suited to highly nonlinear problems. Through its C++ plug-in option, it allows implementation of User-Defined-Models (UDMs) that allow for the accurate simulation of complex soil response patterns like the ones expected herein. Finally, it incorporates various types of structural elements which are necessary for the simulation of the buckets and the jacket.

The 3D numerical model built for the simulation of the problem is shown on Figure 2a while Figure 2b shows a vertical cross section of the model through the center of buckets A and B. The three buckets have a diameter over length ratio *D/L*=1.25.

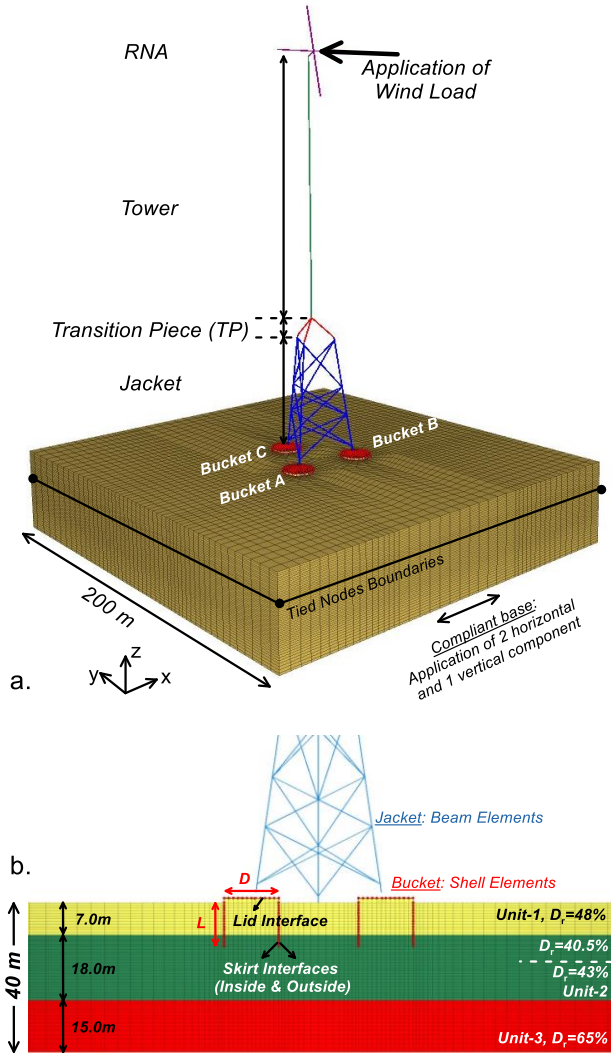

Figure 2. 3D numerical model

The base of the model was subjected to three-directional (two horizontal and one vertical) dynamic loading. Figure 3 shows time histories of the three acceleration components normalized with the corresponding peak values. A compliant base was used at the bottom of the model, while tied-nodes were used for the lateral boundaries. The specific type of constraint forces all gridpoints of a given elevation to move together.

Each analysis was performed in three steps: (a) Gravitational equilibrium of a wished-in-place structure, (b) Application of a static horizontal force at the RNA node and oriented towards suction bucket C (Figure 2a) representing the thrust force on the RNA

during operational conditions, and (c) Application of the earthquake motions at the base of the model.

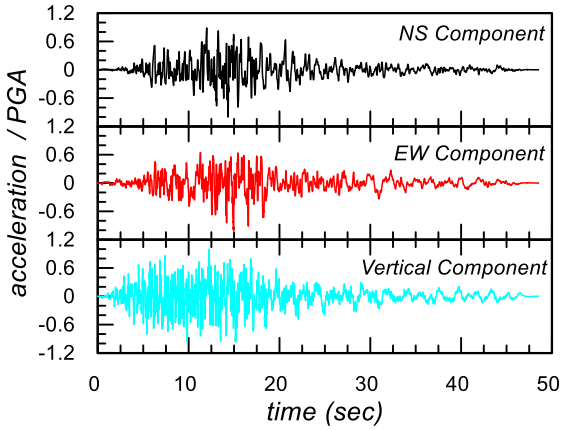

Figure 3. Time histories of the normalized horizontal and vertical acceleration components applied at the base of the model

3.1 Suction buckets and Interfaces

The suction buckets were simulated with isotropic, linear elastic shell elements Young's modulus E=210GPa and Poisson's ratio v=0.25 which constitutes a lower bound for steel. Interface elements characterized by Coulomb sliding and tensile separation were used below the bucket lid and along the inner and the outer part of the skirt. The interface friction angle was set equal to 29°. The tensile strength was set equal to zero at the skirt interfaces and equal to the suction pressure of the water at that depth at the lid interface to ensure that separation will occur if the water below the lid cavitates.

3.2 Jacket, Tower and RNA

The jacket, the transition piece and the wind turbine tower were simulated with linear elastic beam elements. The connections between the jacket and the bucket lid, the jacket and the transition piece as well as the transition piece and the tower were assumed rigid. The total mass of the jacket and the tower, which includes the self-weight of the steel structure, some extra lumped masses due to appurtenances, as well as the hydrodynamic masses for the submerged part of the jacket, was simulated by means of an equivalent uniform density assigned on the beam elements. The inertial properties were properly calibrated to capture the inertial characteristics of the structure. The beams comprising the transition piece were assumed rigid. The beams comprising the RNA were properly calibrated to capture both the RNA mass as well as the moment of inertia due to the rotating blades.

3.3 Constitutive models

The Ta-Ger constitutive model (Tasiopoulou & Gerolymos, 2016b, 2016a) was used to model sand behaviour. Ta-Ger is as a bounding single-surface model, within a smooth hysteresis framework. Its terms are based on a parameter ζ which is defined as the ratio of the current stress to the bounding surface, thus, ensuring that it is always bounded within the range [0,1]. The parameter ζ is raised to the evolving hardening exponent, n which controls the level of nonlinearity. The model is combined with Bolton's dilatancy index, I_R, (Bolton, 1986) and Rowe's plastic flow rule for cohesionless soils (Rowe, 1962), to facilitate capturing the full range of sand behaviour under monotonic/cyclic and drained/undrained loading conditions with a unique set of model parameters. Characteristic behaviours that are captured include soil hardening, softening, densification and shakedown effects as well as static and cyclic liquefaction. The model has been implemented in FLAC3D and its performance has been extensively validated against different types of problems including earthquake-related applications like the one addressed herein (Chaloulos et al., 2023; Tasiopoulou et al., 2023).

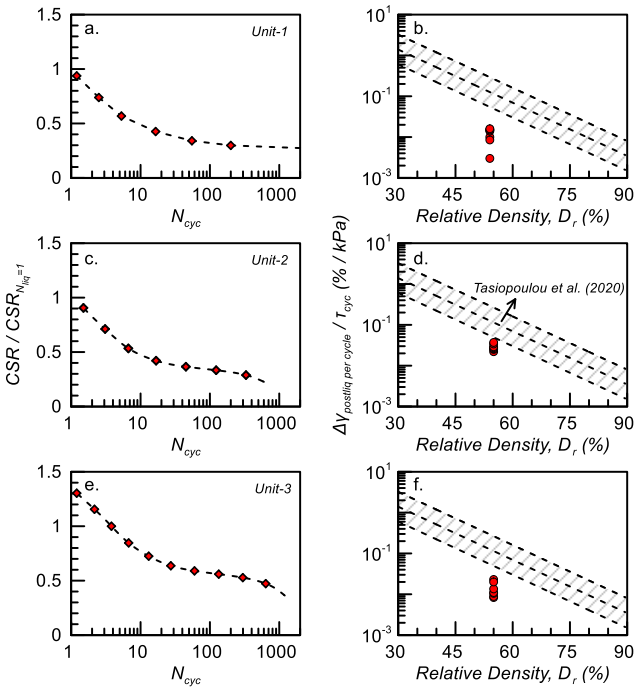

Figure 4. Ta-Ger calibration

Figure 4a, Figure 4c and Figure 4e present the liquefaction triggering curves of the calibrated Ta-Ger model parameters for Unit-1, Unit-2 and Unit-3 respectively. Furthermore, Figure 4b, 4d and 4f present the corresponding numerical post-liquefaction shear strain accumulation rate estimates. Also plotted

on the same figures are the semi-empirical relationships of the compliance rate (i.e., the post-liquefaction shear strain rate per cycle over the shear stress amplitude as a function of the relative density of the soil) proposed by (Tasiopoulou et al., 2020). Finally, Figure 5 presents typical results from single element numerical siumulations of undrained CSS tests in terms of normalized shear stress (CSR) and normalized vertical stress as well as CSR and shear strain for soil samples from Unit-1 and Unit-2 (Figure 4a and 4b respectively). Notice that in the latter case of silts the normalized vertical stress in the tests does not reach a value of zero signifying that complete liquefaction is avoided.

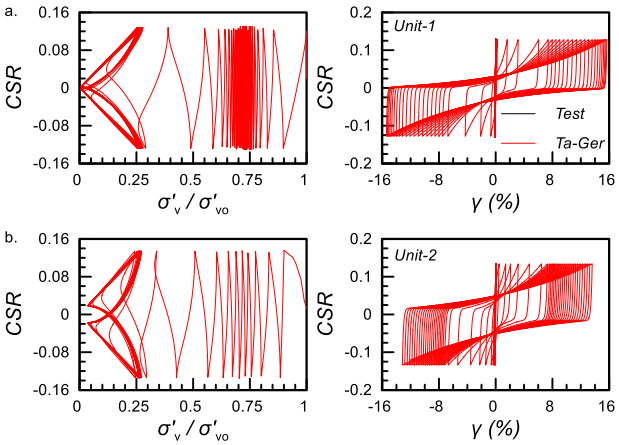

Figure 5. Typical comparisons between experimental data and single element simulation for Unit-1 and Unit-2.

4 EVALUATION OF SBJ PERFORMANCE

4.1 Soil response

Figures 6a and 6b show contours of excess pore pressure ratio at the end of shaking along a vertical cross-section passing through the center of buckets A and B and along a vertical cross-section through the center of buckets A and C, respectively. As shown on the figure, extensive liquefaction (signified by excess pore pressure ratio values of $r_u \approx 1$) occurs within the largest part of Unit-1 and Unit-2. It is noteworthy, however, that the area directly below the buckets attains r_u values significantly lower signifying only partial liquefaction. This type of response has been widely observed for shallow footings founded on liquefiable soils and is attributed both to the large confinement provided by the vertical load of the structure as well as to shear-induced dilation as a result of the accumulated settlement (Bullock et al., 2019; Chaloulos et al., 2020; Macedo & Bray, 2018). Note that the size of this zone is larger and the associated r_u values are lower below bucket C as a result of the higher initial pre-shaking vertical compression load (due to the application of the static wind force, Figure 2a). The formation of these zones is a key response aspect as it prevents total loss of shear strength and subsequently foundation failure.

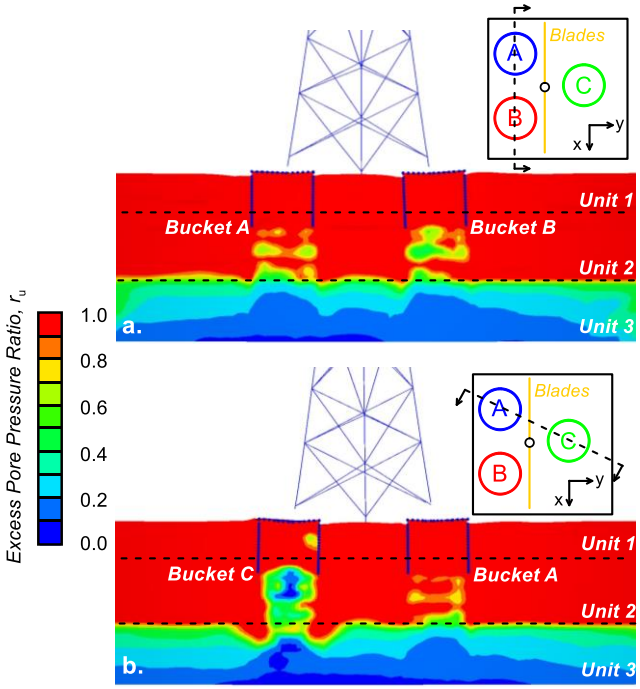

Figure 6. Contours of Excess Pore Pressure ratio r_u at the end of shaking along two vertical cross-sections

4.2 Bucket response

The performance of the bucket foundations is evaluated on Figure 7a and 7b which show time histories of settlements and horizontal displacements along the x- and y- direction respectively for buckets A, B and C (blue, red and green line respectively) whose location relative to the WTG is illustrated in the inset of Figure 6a. The horizontal displacement is practically uniform for all three buckets however Bucket C accumulates slightly more settlement as a result of the higher initial (pre-shaking) compressional vertical load. The residual foundation settlement is approximately 1.3-1.7% of the bucket diameter for buckets A and B, and approximately 2.0% for bucket C. The corresponding horizontal displacement is in the order of 1.0-1.5% for both x- and y- direction.

Figure 8 presents time histories of differential settlements between the edges of the bucket. Along the y- direction (Figure 8a) maximum differential settlements occur at bucket C with peak and residual values of around 0.15 and 0.08 m respectively. Along the x-direction (Figure 8b) maximum rotations occur at bucket B with a peak value of approximately 0.14 m occurring at the end of shaking.

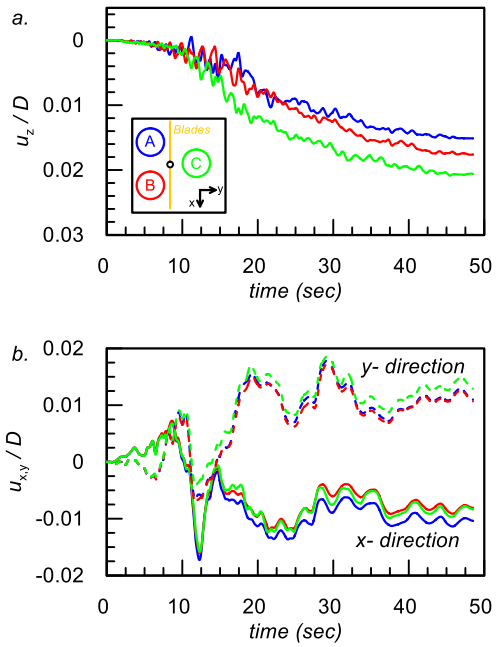

Figure 7. Time histories of settlements and horizontal displacements of the three buckets

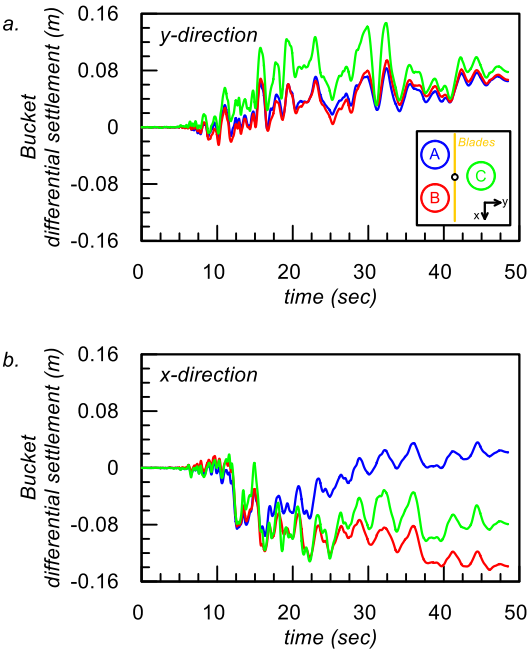

Figure 8. Time histories of bucket differential settlements along the (a) y- and (b) x-direction

4.3 WTG response

The response of the Wind Turbine Generator (WTG) is evaluated on Figure 9a and 9b in terms of Side-Side and Fore-Aft differential settlement, and horizontal x- and y- displacement at the RNA respectively. Side-Side differential settlement is defined as the differential settlement between buckets A and B (see inset of Figure 9b) while Fore-Aft rotation is defined as the differential settlement between bucket C and the average between buckets A and B. The maximum differential settlement occurs in the fore-aft direction with peak and residual values of 0.05 and 0.03 m, respectively. Similarly, maximum horizontal displacements accumulate in the y-direction (the direction along which the wind load is applied) with a maximum and residual value of approximately 5.0 and 4.0% of the bucket diameter *D* respectively.

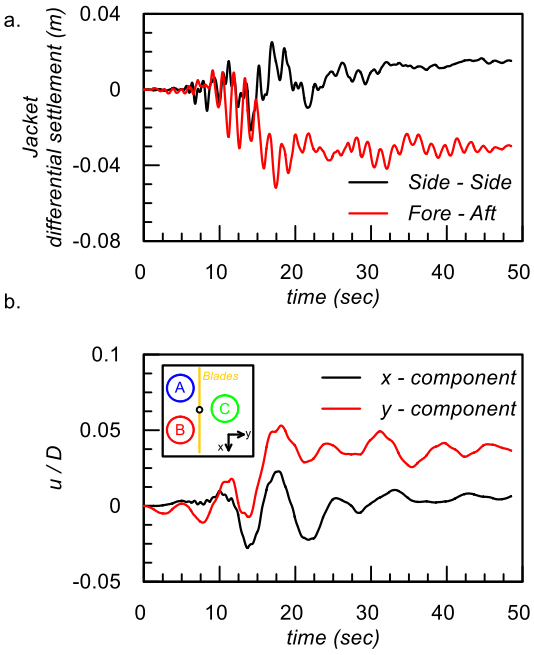

Figure 9. Time histories of (a) WTG side-side and fore-aft differential settlements and (b) horizontal displacement at the RNA

5 CONCLUSIONS

The paper presented the development and application of a novel 3D numerical methodology, as part of a technical project, for the analysis of a three-leg Suction Bucket Jacket (SBJ) built on a liquefiable seabed. The methodology explicitly simulated the jacket through properly calibrated beams, the buckets, the Soil-Foundation interaction as well as the complex response of the soil units under earthquake-induced dynamic loading using the Ta-Ger constitutive model.

Analyses results showed that significant development of excess pore pressures can occur within the foundation soil, thus leading to displacement and rotation accumulation both at foundation level and structure. However, for the SBJ design analysed, a zone of limited excess pore pressure build-up is formed around the tip of the buckets which results in limited displacement accumulation. The study showed that even if simplified methods suggest that significant excess pore pressures may develop within the foundation soils, only the adoption of a performance-based context can demonstrate whether its consequences are significant for the stability and

operation of the OWT. The ability to use appropriately calibrated and validated constitutive models that can capture all relevant aspects of soil cyclic response, and efficiently simulate soil-structure interaction effects was thus invaluable.

AUTHOR CONTRIBUTION STATEMENT

All Authors: Software, Conceptualization, Methodology, Investigation, Writing-Original draft, Writing-Reviewing and Editing,

REFERENCES

Andrus, R. D., Mohanan, N. P., Piratheepan, P., Ellis, B. P., & Holzer T L. (2007). Predicting shear-wave velocity from cone penetration resistance. In: *4th Int Conf Eq Geot Eng., Thessaloniki, Greece*

Bolton, M. D. (1986). The strength and dilatancy of sands. *Géotechnique*, *36*(1), 65–78. 10.1680/GEOT.1986.36.1.65

Boulanger, R. W., & Idriss, I. M. (2014). *CPT and SPT Based Liquefaction Triggering Procedures, Report No. UCD/CGM-14/01*.

Bullock, Z., Karimi, Z., Dashti, S., Porter, K., Liel, A. B., & Franke, K. W. (2019). A physics-informed semi-empirical probabilistic model for the settlement of shallow-founded structures on liquefiable ground. *Géotechnique*, *69*(5), 406–419. 10.1680/jgeot.17.P.174

Chaloulos, Y. K., Giannakou, A., Drosos, V., Tasiopoulou, P., Chacko, J., & de Wit, S. (2020). Liquefaction-induced settlements of residential buildings subjected to induced earthquakes. *SDEE*, *129*. 10.1016/j.soildyn.2019.105880

Chaloulos, Y. K., Tasiopoulou, P., Georgarakos, T., Giannakou, A., Chacko, J., & Unterseh, S. (2023). 3D Effective stress analyses of dynamic LNG tank performance on liquefiable soils improved with stone columns. *SDEE*, *174*. 10.1016/J.SOILDYN.2023.108170

Farahani, S., & Barari, A. (2023). A simplified procedure for the prediction of liquefaction-induced settlement of offshore wind turbines supported by suction caisson foundation based on effective stress analyses and an ML-based group method of data handling. *Eq Eng & Str Dyn*, *52*(15), 5072–5098. 10.1002/EQE.4000

Gao, B., Ye, G., Zhang, Q., Zhu, W., & Zhang, L. (2023). Seismic responses of suction bucket foundation in liquefiable seabed considering spatial variability. *COGE*, *159*. 10.1016/J.COMPGEO.2023.105495

Gao, B., Zhu, W., Zhang, Q., & Ye, G. (2022). Response of suction bucket foundation subjected to wind and earthquake loads on liquefiable sandy seabed. *SDEE*, *160*. 10.1016/J.SOILDYN.2022.107338

Itasca. (2019). *FLAC3D - Fast Lagrangian Analysis of Continua in Three-Dimensions, Ver. 7.0*. Itasca Consulting Group Inc.

Macedo, J., & Bray, J. D. (2018). Key Trends in Liquefaction-Induced Building Settlement. *J Geot and Geoenv Eng*, *144*(11). 10.1061/(ASCE)GT.1943-5606.0001951

Robertson, P. K. (2010). Soil Behaviour Type from the CPT: An Update. In: *2nd Int. Symp. on Cone Penetration Testing, Huntington Beach, CA, USA, Vol. 2, 575-583*.

Rowe, P. (1962). The stress-dilatancy relation for static equilibrium of an assembly of particles in contact. *Proceedings, Royal Soc.*

Tasiopoulou, P., Chaloulos, Y. K., Giannakou, A., & Chacko, J. (2023). Seismic performance of sheet-pile wall supporting liquefiable backfill: Blind predictions of centrifuge model tests using Ta-Ger constitutive model. *SDEE*, *174*. 10.1016/J.SOILDYN.2023.108174

Tasiopoulou, P., & Gerolymos, N. (2016a). Constitutive modeling of sand: Formulation of a new plasticity approach. *SDEE*, *82*, 205–221. 10.1016/J.SOILDYN.2015.12.014

Tasiopoulou, P., & Gerolymos, N. (2016b). Constitutive modelling of sand: a progressive calibration procedure accounting for intrinsic and stress-induced anisotropy. *Géotechnique*, *66*(9), 754–770. 10.1680/JGEOT.15.P.284

Tasiopoulou, P., Ziotopoulou, K., Humire, F., Giannakou, A., Chacko, J., & Travasarou, T. (2020). Development and Implementation of Semiempirical Framework for Modeling Postliquefaction Shear Deformation Accumulation in Sands. *J Geot and Geoenv Eng*, *146*(1). 10.1061/(ASCE)GT.1943-5606.0002179

Ueda, K., Uzuoka, R., Iai, S., & Okamura, T. (2020). Centrifuge model tests and effective stress analyses of offshore wind turbine systems with a suction bucket foundation subject to seismic load. *Soils and Foundations*, *60*(6), 1546–1569. 10.1016/j.sandf.2020.08.007

Yu, H., Zeng, X., & Lian, J. (2014). Seismic behaviour of offshore wind turbine with suction caisson foundation. In: *Geo-Congress 2014, Atlanta, Georgia, USA*.